# BEAM INDUCED FLUORESCENCE MONITOR - SPECTROSCOPY IN NITROGEN, HELIUM, ARGON, KRYPTON AND XENON GAS

F. Becker*, P. Forck, T. Giacomini, R. Haseitl, B. Walasek-Hoehne, GSI, Darmstadt, Germany

F.M. Bieniosek, P.A. Ni, LBNL, Berkeley, California, D.H.H. Hoffmann, TU-Darmstadt, Germany

*Abstract*

As conventional intercepting diagnostics will not withstand high intensity ion beams, Beam Induced Fluorescence (BIF) profile monitors constitute a pre-eminent alternative for non-intercepting profile measurements [1]. This diagnostic technique makes use of the optical fluorescence emission of beam-excited gases. Recently BIF became an important diagnostic tool for transversal beam profile measurements with applicability in beam tuning over a wide range of beams and accelerator conditions [2]. In this paper optical VIS-spectroscopy with an imaging spectrograph for 5 MeV/u proton, $S^{6+}$ and $Ta^{24+}$ beams in nitrogen, Xe, Kr, Ar, Ne and He at $10^{-3}$ mbar gas pressure is presented. Atomic physics processes are a major performance issue, since they determine transition intensities and lifetimes of excited states. Further investigations are required to improve the detector performance and increase its range of application.

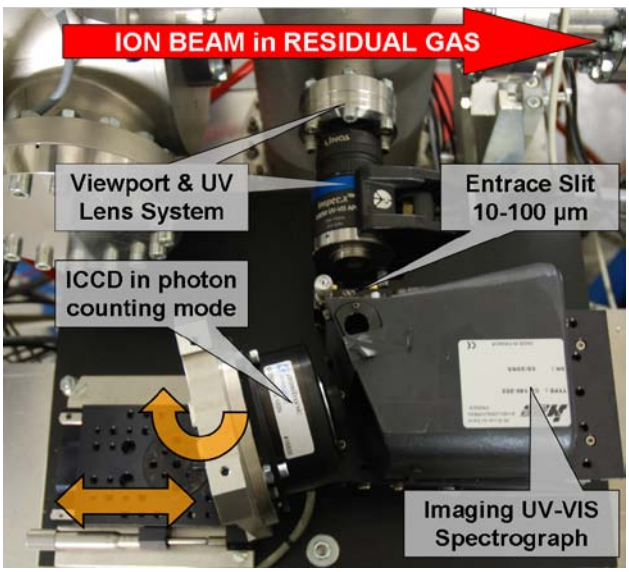


Figure 1: Top-view of the optical setup looking onto the diffractive plane. Length of spectrum in the image plane is 10 mm. 1:1 imaging from slit to image plane. All refractive optics adapted to UV-VIS [4]. ICCD performs single photon detection including a Ø 25 mm UV-enhanced photocathode with a V-stack MCP [5] and digital VGA 8-bit greyscale camera [6].

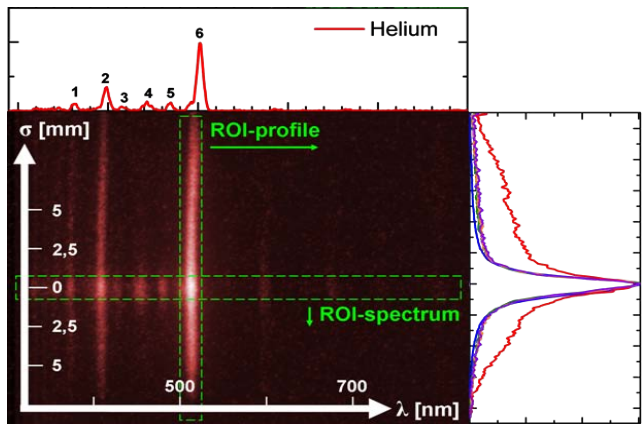


Figure 2: Spectrographic average image of n=2000 pulses of $3{\cdot}10^{11}$ $S^{6+}$ ions @ 5.16 MeV/u in $10^{-3}$ mbar helium gas, $\sigma_w$=1.8 mm. Log colour-scale for better illustration. Projections yield either spectra (upper) or profiles (right).

## EXPERIMENTAL SETUP

Key issue of this experimental layout using an imaging spectrograph with an area scan intensified CCD (ICCD) camera (Fig. 1) was to have both, the spectral information of specific beam induced gas transitions along the diffraction axis and the spatial information about the beam profile width, transition wise along the imaging axis, see Figure 2. For 150 mm object distance, a chromatically corrected UV-lens of f = 50 mm and f/2.8 was chosen. A CCD height of 4.9 mm and a total reproduction scale $\beta_{tot}$ = 0.42 yield a 19.5 mm field of view, covering ~ $5{\cdot}\,\sigma_w$.

### *Imaging Spectrograph & Gas Composition*

The spherical mirror (Ø 70 mm) with 140 mm focal length is holographically etched and astigmatism corrected. 140 sinusoidal grooves per mm produce a spectral dispersion of 50 nm/mm and an image field of 8x12 mm on the vertical imaging axis and the horizontal dispersive axis, respectively. With an optical resolution of 33 lp/mm the ICCD limits the spectral resolution to 1.5 nm for an entrance slit ≤ 30 µm. The total spectral system efficiency includes all single component efficiencies as a convolution, see Fig. 3 (upper plot). Most limiting factors for increasing wavelength ≥ 600 nm are the tri-alkali $(Na_2KSb)Cs$ photocathode and the decreasing grating-efficiency. Investigation of optical gas spectra relies on a

* Frank.Becker@gsi.de

sufficient purity of the actual gas species.

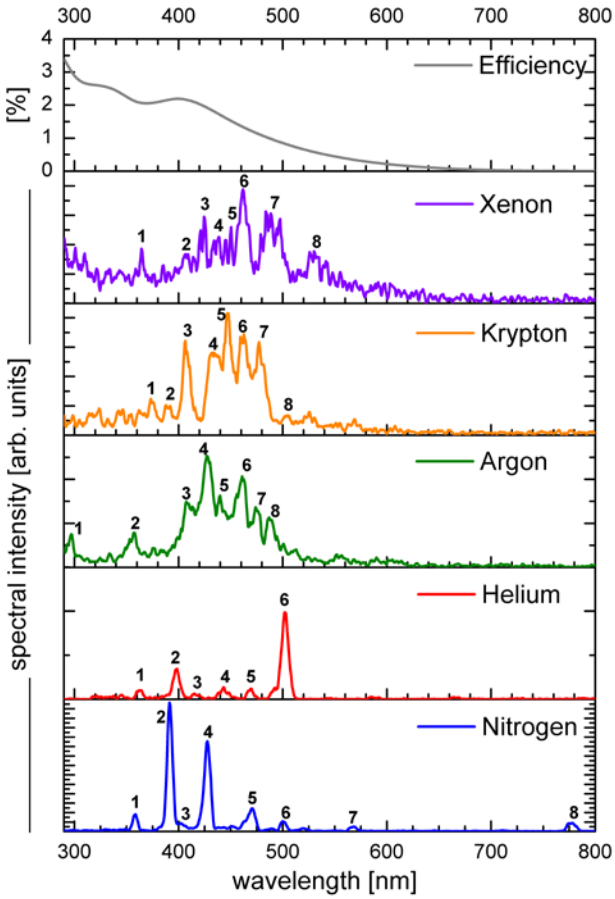


Figure 3: Optical Beam Induced Fluorescence spectra of $3{\cdot}10^{11}$ $S^{6+}$ ions @ 5.16 MeV/u in $10^{-3}$ mbar residual gases (Xe, Kr, Ar, He, $N_2$). Most prominent transitions are indicated and described in Table 1. The total spectral efficiency in the upper plot is determined by single efficiencies of the lens, grating and photocathode.

In order to measure and control impurities, a residual gas analyzer (RGA) 'quadrupole mass spectrometer'-type was used [7]. Base pressure of the unbaked vacuum system was $10^{-7}$ mbar, with the typical fingerprint of hydrogen, water, nitrogen and traces of the previously introduced rare gas species like krypton in an argon atmosphere. Although the gas leak system was flushed carefully after each gas exchange, a significant source of residuals was gas contamination the pressure reducing regulator. In order to keep relative impurities below 5 %, the working pressure for all experiments had to be set to $10^{-3}$ mbar $N_2$-equivalent. More details about that in [9].

## DATA ANALYSIS – RESULTS

All optical spectra were recorded during 2000 beam pulses for constant accelerator settings. Each single image was recorded as 8-bit bitmap, using the ICCD in photon counting mode. To maintain the dynamic range, the average images were 32-bit float tiffs, see Fig. 2. Further resolution improvement by a factor of ~ 4 was achieved with a cognitive algorithm that determined barycenters of single photon spots and added them as single counts to the VGA-sized matrix [8]. To discriminate spectral peaks against spiky shot noise, Savitzky-Golay fits were applied. Regions of interest (ROI) were chosen like 10 pixel or 40 µm at the beam center for the BIF-spectra in Fig. 3 and like 20 pixel or 16 nm for the transitions specific profile plots in Fig. 4 (mid & bottom).

Table 1: Residual gases (block-wise), observed charge states, observed integral intensity $I_{meas}$, $I_{gas}$ normalized to $p_{eff}$ and $I_{gas\&Z}$ normalized to $p_{eff}$ and Z (upper block line). Corresponding transitions as indicated in Figure 3, central wavelength and relative intensity with respect to the integral intensity (lower block line). Peaks indicated with No.)* are superpositions of several transition-lines.

| **gas species** | **Charge state** | **$I_{meas}$ $I_{gas}$ $I_{gas\&Z}$** |
|---|---|---|
| **No.)** central-wavelength [nm], *relative intensity [%]* | | |
| **Xenon** | **$Xe^+/Xe$** | **41; 86; 22** |
| **1)** 363, *4*; **2)*** 407, *4*; **3)*** 424, *6*; **4)*** 438, *5* | | |
| **5)** 450, *2*; **6)*** 462, *12*; **7)*** 484, *16*; **8)*** 530, *5* | | |
| **Krypton** | **$Kr^+/Kr$** | **45; 63; 25** |
| **1)** 373, *4*; **2)*** 388, *3*; **3)** 407, *10*; **4)*** 434, *14* | | |
| **5)** 447, *12*; **6)*** 463, *12*; **7)*** 477, *13*; **8)*** 505, *2* | | |
| **Argon** | **$Ar^+$** | **50; 38; 30** |
| **1)** 297, *3*; **2)**_ 357, *5*; **3)**_ 407, *11*; **4)** 427, *19* | | |
| **5)*** 440, *8*; **6)*** 461, *15*; **7)*** 474, *8*; **8)*** 487, *7* | | |
| **Helium** | **He** | **21; 4; 26** |
| **1)** 364, *4*; **2)** 398, *16*; **3)*** 415, *3*; **4)*** 443, *7* | | |
| **5)*** 470, *5*; **6)** 502, *48* | | |
| **Nitrogen** | **$N_2^+/N^+$** | **100; 100; 100** |
| **1)** 358, *4*; **2)*** 391, *45*; **3)*** 428, *29*; **4)*** 470, *9* | | |
| **5)** 501, *3*; **6)** 560, *1*; **7)*** 776, *3* | | |

### *BIF-Spectra*

All spectra were first calibrated to an Hg-Ar-standard and then refined step by step adding identified transitions of the recorded BIF-spectra. The accuracy for the central wavelength is ≤ 1 nm. The investigations were performed with 5 ms long beam pulses of $3{\cdot}10^{11}$ $S^{6+}$ ions at 5.16 MeV/u, focused to a $\sigma_w$ = 1.8 mm. Obtained BIF spectra are depicted in Fig. 3. Actual spectra have not been normalized to the spectral efficiency of the optical components, which is therefore given in Fig. 3 as well (upper-plot). In Table 1 the observed charge states, relative integral intensities and most prominent transitions are listed. Different signal-to-noise ratios for the gas species are determined by the observed integral intensity I. Spectral lines of optical transitions in nitrogen and helium are pronounced and more clearly separated as compared to the heavier rare gas species, showing many clustered lines of lower intensities. Although nitrogen shows the brightest transitions, e.g. xenon and krypton

show similar integral intensities $I_{gas}$, normalized with respect to effective gas pressure $p_{eff}$.

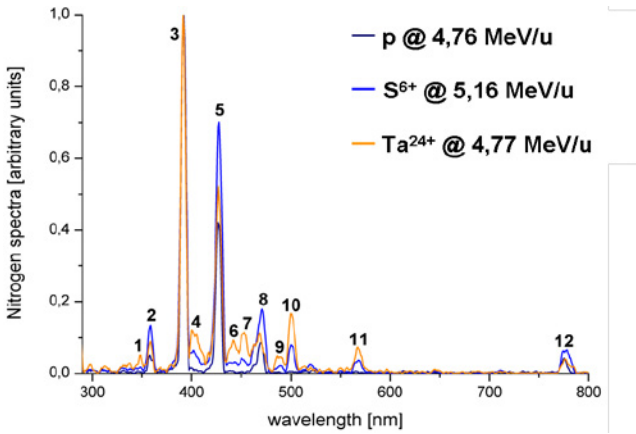


Figure 4: Comparison of nitrogen spectra induced by different ion species (p, $S^{6+}$, $Ta^{24+}$) of the same energy. The heavier the ion ($Ta^{24+}$), the more intense transitions of singly dissociated singly charged nitrogen atoms appear.

To account for the electronic stopping power, integral intensities $I_{gas\&Z}$ were furthermore normalized to Z. This intensity represents a fluorescence-efficiency normalized to the differential energy loss -dE/dx. $I_{gas\&Z}$ of all rare gas species is similar, except for nitrogen having a four times higher fluorescence-efficiency. In contrast to the other gases with ionic transitions, He-fluorescence is caused by transitions of the neutral atom, see Tab. 1. Ion species and charge states influence the dissociation probability of $N_2$, since additional atomic lines appear for heavy ions, see Fig. 4. When the ROI was moved from the profile center to the beam fringes, spectral intensity decreased for all gases in the same way, except for helium that showes an unequal decrease for different transitions.

### *Transition dependent Profile Data*

Motivated by the abnormality of He-spectra, profile plots were recorded for beam conditions of Figure 3, as spectrally integrated profiles (see Fig. 5), or transition-wise [13]. To be able to compare the profiles, they have been normalized to their maximum specific intensity. All gas-species show similar profile widths $\sigma_w$ besides helium, showing a factor of 2.5 larger $\sigma_w$. Assuming that neutral He atoms might have large cross-sections for electron excitation, an 8 mm beam halo is reasonable, as the mean free path of secondary electrons is in the order of 10 mm, for $p_{eff} = 4 \cdot 10^{-3}$ mbar. For proton beams as well as for Ta and U beams, similar spectra and profiles were obtained.

## CONCLUSION

Optical spectra of nitrogen, xenon, krypton, argon and helium were successfully recorded. They excellently agree with measurements at lower beam energies ≤ 10 MeV/u in the case of nitrogen [10, 11] and higher beam energies in the range of 50 MeV/u to 25 GeV/u for nitrogen and xenon [12]. The present experiments show hat nitrogen is the most appropriate residual gas for BIF applications, because of its spectral concentration between 390 and 430 nm, fitting typical S20-cathode efficiencies. In addition, nitrogen shows the highest integral intensity. Especially the four times higher fluorescence-efficiency $I_{gas\&Z}$ makes it the right choice, if stopping power is an issue. Intense ion beams can generate electric fields in the order of 10 kV/mm, so that trajectories of excited charged molecules like $N_2^+$, are influenced by the beam's space charge and perturb the profile reading [13]. Therefore different selection criteria come into play, like e.g. larger molecule masses and shorter transition-lifetimes, provided by rare gases like Xe and Kr. Helium is no alternative due to its wrong profile image in the considered pressure range. Once a residual gas is selected, optical components like lenses or photo-cathodes have to be further optimized. However, the outcome of our experiment is, that for most beam parameters $N_2$ is the optimal choice.

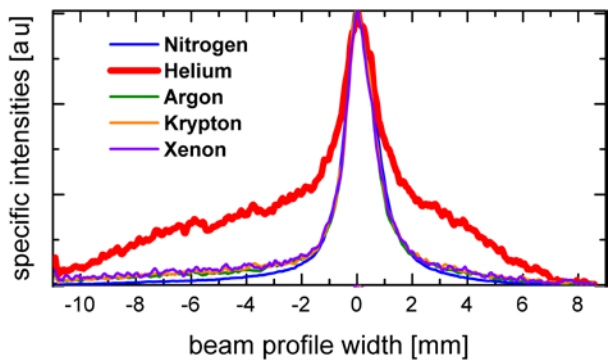


Figure 5: Optical Beam Induced Fluorescence spectra of $3 \cdot 10^{11}$ $S^{6+}$ ions @ 5.16 MeV/u in $10^{-3}$ mbar residual gases (Xe, Kr, Ar, He, N2). Most prominent transitions are indicated and described in Table 1. The total spectral efficiency in the upper plot is determined by the lens, grating, and photocathode.

## REFERENCES

[1] P. Forck et al., DIPAC'05, ITTA01, 2005.
[2] F. Becker et al., DIPAC'07, MOO3A02, 2007.
[3] Company: www.horiba.com, CP140202 spectrograph.
[4] Company: www.linos.com, inspec.x 2.8/50 UV-VIS apochromatically corrected lens system.
[5] Company: www.proxitronic.de, BV-2581 QYV 100N.
[6] Company: www.baslerweb.com, Type 311-f VGA Sony ICX414AL Sensor.
[7] Company: www.pfeiffer-vacuum.de, Gauge PKR-261, Valve EVR-116, Controller RVC-300, Calibration-Gauge CMR-264, RGA PrismaPlus.
[8] Software: http://rsbweb.nih.gov/ij/, Image-J package.
[9] F. Becker, "Non-destructive Profile Measurement of intense Ion Beams", PhD-thesis, Darmstadt, 2009.
[10] R.H. Hughes et al., Phys. Rev., 123, 2084 (1961)
[11] C. S. Lee et al., "Study of N2+ first negative system" Nucl. Instrum. Meth. B 140, p. 273-280, 1998.

[12] M. A. Plum et al., “N2 and Xe gas scintilliation @ Cern PS and Booster”, Nucl. Instrum. Meth. A 492, p. 74-91, 2002.
[13] F. Becker et al., BIW’08, California , 2008.